Journal of Alloys and Compounds, *188* (1992) 198–201
JALCOM 9028

On three-dimensional defects in the $Ni_3Al(\gamma')$ phase identified by the computed imaging technique

R. Bonnet
Institut National Polytechnique, LTPCM–ENSEEG, Domaine Universitaire, BP 75, 38402 Saint Martin d'Hères (France)

A. Ati
Institut de Génie mécanique, USTHB, BP 32, El-Alia, Bab-Ezzouar, Algiers (Algeria)

D. David
Institut National Polytechnique, LTPCM–ENSEEG, Domaine Universitaire, BP 75, 38402 Saint Martin d'Hères (France)

Abstract

Despite the large number of studies on the plastic properties of $L1_2$ crystals, the crystalline defects produced by high temperature deformation of phases based on $Ni_3Al(\gamma')$ are not yet thoroughly understood. Some examples of unusual three-dimensional defects have been observed in deformed γ' precipitates of the industrial nickel-based two-phase superalloy CMSX2 and in deformed specimens of the $L1_2$ alloy 9Al–14Ti–3.5Cr–73.5Ni (atomic per cent). These defects, which involve superlattice stacking faults, stair-rod-dislocation-like defects and superpartial dislocations, are analysed by both conventional and high resolution electron microscopy, and the computed imaging technique coupled with two-beam diffraction theory.

1. Introduction

In the last few years, studies devoted to the study of plastic deformation of nickel-based two-phase superalloys used for turbine blade materials have mentioned the presence, inside the γ' precipitates and at the γ–γ' interface, of partial dislocations bordering antiphase boundaries (ABs) and planar faults. As shown below, the physical mechanisms related to the shearing process of the γ–γ' interface and to the dislocation glide in the γ' precipitates can also generate complex three-dimensional crystalline defects if the plastic deformation is severe. Examples of complex defects produced from hot plastic deformation were first given by Huis in't Veld *et al.* [1] who observed stair-rod-dislocation-like (SRDL) defects and thin twins in γ' precipitates. However, their weak beam experiments could not describe unambiguously the details of the SRDL defect structures. Other unusual defects were also observed by Bonnet and Derder [2], formed by interacting ABs, superlattice intrinsic stacking faults (SISFs) and superlattice extrinsic stacking faults (SESFs) as described by Pope and Ezz [3].

In this paper we detail an investigation by transmission electron microscopy (TEM) on the structures of such three-dimensional defects whose role in work hardening is unknown at present. Complementary techniques have been used such as the dark field imaging method [4], high resolution TEM, and the computed imaging technique [5] based on two-beam diffraction theory. All the geometry and crystallography of the defects have been determined with the aid of the software METPACK [6]. Theoretical images are calculated within the assumption of the two-beam theory.

2. Planar defects and stair-rod dislocations in plastically deformed γ'

Figure 1 depicts a typical area of a deformed single grain of the industrial two-phase superalloy CMSX2, deformed by compression (900 °C, 1%, 3.3 mm s^{-1}). Planar defects looking like SISFs or SESFs are identified in the γ' precipitates (composition 16.7Al–1.7Ti–3.8Cr–70.8Ni–3.5Co–1.1Ta–2.6W, in atomic per cent [7]) from the analysis of α fringes. Most of them are limited at γ–γ' interfaces by dislocations whose contrast behaviour corresponds to those of Shockley partials $(1/6)\langle 112\rangle$, as shown in refs. 8–10. The extension of each planar defect inside a γ' precipitate can be limited by a superpartial dislocation $(1/3)\langle 112\rangle$, or from place to place by another crossing planar defect or an SRDL defect. In our sample, the contrasts of most of the planar defects behave like that of SESFs, or less commonly, SISFs. Figure 2 shows an unusual interaction between two superpartials gliding on different but parallel $(1\bar{1}\bar{1})$

0925-8388/92/$5.00

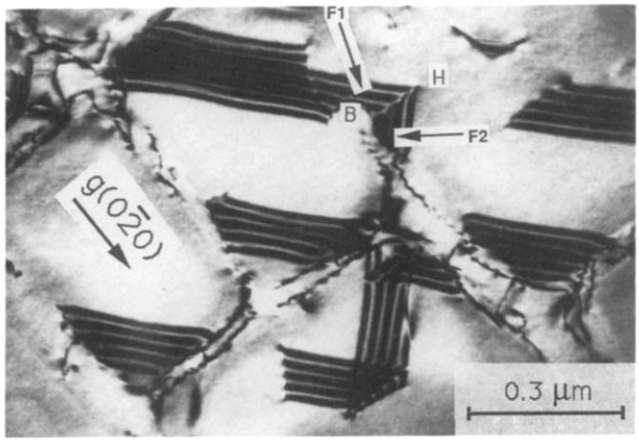

Fig. 1. Bright field image of a CMSX2 superalloy single grain plastically deformed at 900 °C. Electron beam parallel to [001]. F1 and F2 are two planar defects meeting along the common edge BH.

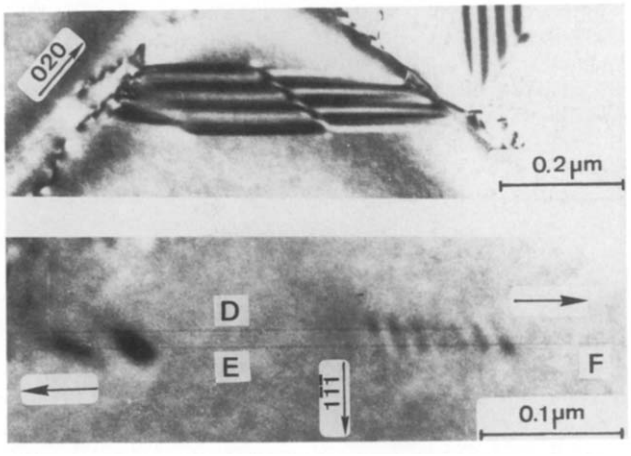

Fig. 2. Bright field images of interacting superpartial dislocations $(1/3)\langle 112\rangle$ which glide along parallel close-packed planes. The planar defects D and E are SISFs while the planar defect F is an SESF. The arrows indicate the sense of the dislocation glides. The spacing between planes D and E is 15 nm. (a) $g(0\bar{2}0)$; (b) $g(1\bar{1}\bar{1})$. Glide traces are apparent from black parallel lines.

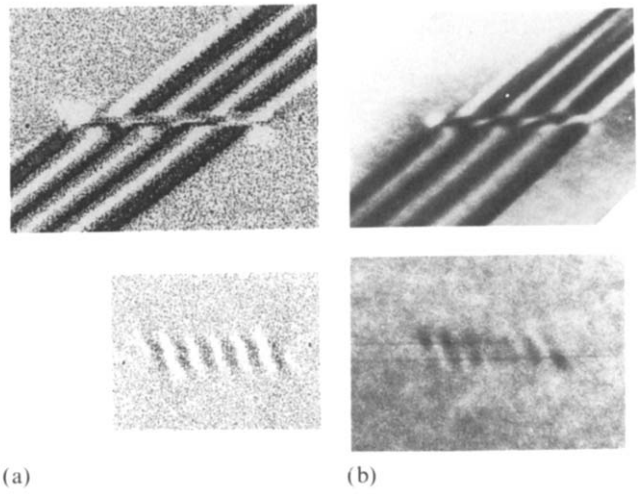

Fig. 3. Identification by the computed imaging technique of the true nature of the faults and of the superpartial dislocation dipole: (a) computed images; (b) experimental images.

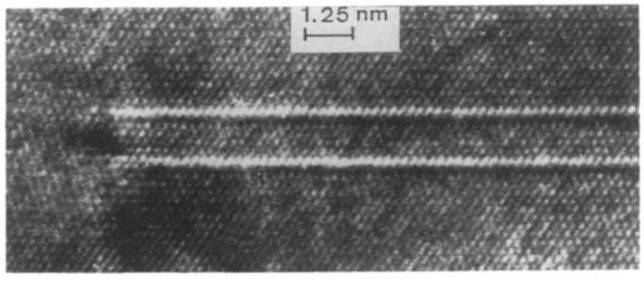

Fig. 4. High resolution TEM image of two elastically interacting superpartial dislocations A and B. These limit the SISFs on the left. The SISFs are six interplanar spacings apart (1.25 nm).

planes. The configuration is in fact a superpartial dipole, identified by the comparison of experimental and computed images (Fig. 3). The upper defect in Fig. 2 is an SISF denoted D, while the lower defect consists in an SISF denoted E followed by an SESF denoted F. The spacing between the two gliding planes, determined by contrast simulations, is about 15 nm. This spacing can be much smaller, as illustrated in Fig. 4, as low as a few interplanar spacings. In this case, the SISFs are only 6 interplanar spacings apart, the gliding superpartials with Burger's vectors $(1/3)\langle 112\rangle$ being in strong elastic interaction. The analysis of such a configuration would have led, in conventional TEM, to an SESF because the spacing is too small to be clearly detected by a change in contrast of the a fringe technique. This question opens therefore the problem of identifying true SESFs and two close and parallel SISFs, or even very thin microtwins, as observed by Huis in't Veld *et al.* [1]. In order to examine this situation, a diffraction experiment was carried out for the same sample as in Figs. 1 and 2, with the aim of examining whether some thin microtwins can exist. The $(1\bar{1}\bar{1})$ plane was oriented edge on (Fig. 5) and the diffraction of thin areas of the foil was observed. This procedure allows the possible diffraction from the largest volume of twinned microcrystals, as well as large rods, to be obtained in reciprocal space. For an orientation very close to $\langle 110\rangle$, some very faint spots can indeed be detected (Fig. 6(a)). The dark field image taken with one of these spots (Fig. 6(b)) proves unambiguously that in the observed area most of the so-called SESFs are indeed very thin microtwins, since the correspondence one by one of the planar defects is clearly visible.

As a conclusion, these observations prove unambiguously that the planar defects which have been studied in

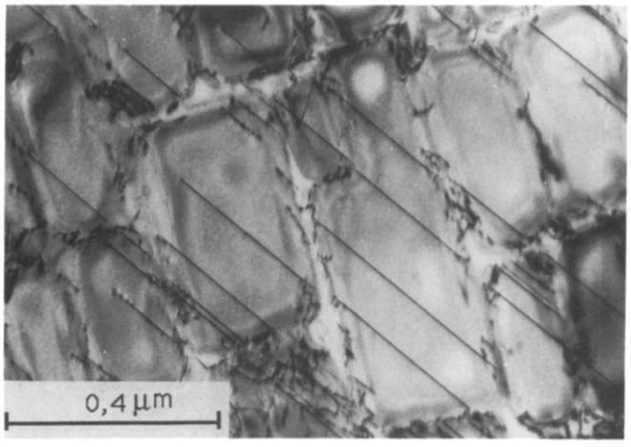

Fig. 5. Bright field image. Defects are seen edge on, parallel to {111} planes.

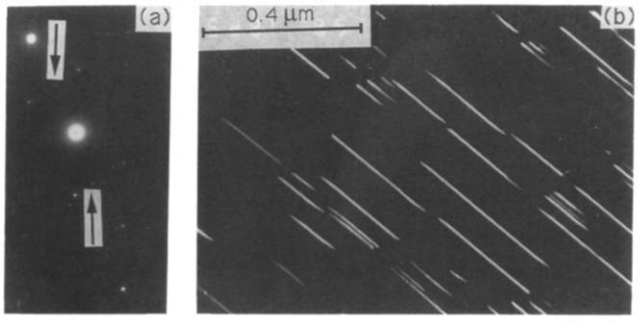

Fig. 6. TEM analysis of planar defects similar to those of Fig. 1. (a) Diffraction pattern with a zone axis close to ⟨101⟩. This contains extra spots due to microtwins, as indicated by arrows. (b) Dark field image revealing the microtwins, formed from the lower extra spot in the diffraction pattern.

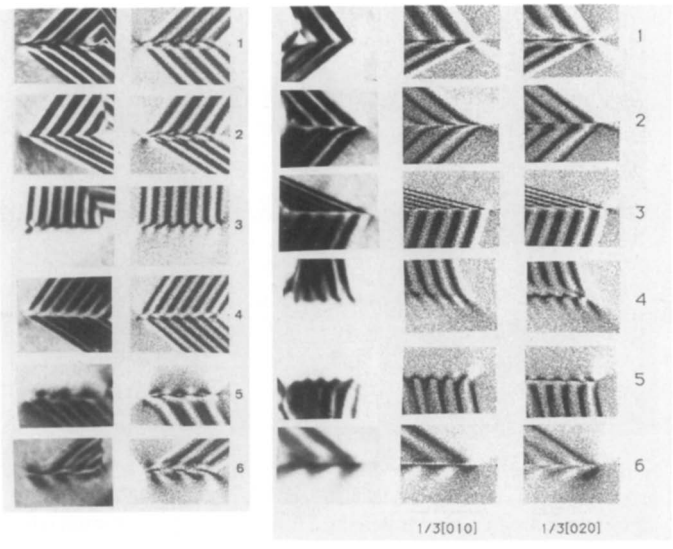

Fig. 7. Comparison between bright field images (columns A and a) and computed images for two kinds of defects. Columns A and B are relative to the true stair-rod dislocation ab in Fig. 8(b), which has an unusually large Burger's vector (1/3)⟨013⟩. Columns a, b, c, are relative to the SRD defect BH in Fig. 1, associated with an elastic field close to a (1/3)⟨010⟩ dislocation as proved by the computed images in column b.

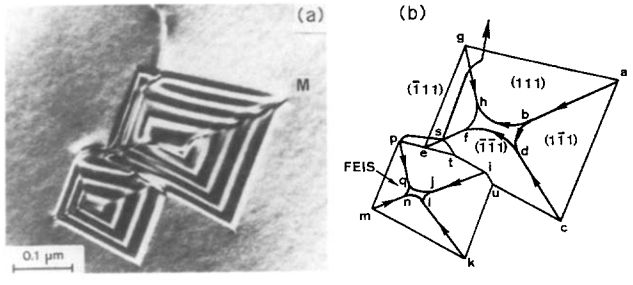

Fig. 8. Pyramids of faults in the plastically deformed alloy 73.5Ni–9Al–14Ti–3.5Cr. (a) Bright field image. (b) All the pyramidal planes are SISFs except the plane mnpq. The stair-rod dislocation ab has the largest Burger's vector ever seen in f.c.c. crystals, *i.e.* (1/3)⟨013⟩.

the past can have structures quite different from simple SISFs or SESFs. In particular, studies in high resolution TEM are needed to understand the true nature of the defects induced by plastic deformation in $L1_2$ crystals (see for example ref. 11).

The problem is to elucidate the nature of the SRDL defect lying at the common edge of two planar SISFs or SESFs. In order to observe within the two-beam approximation the contrasts due to this defect, a search was made for a special alloy whose fault energy is particularly low, which permits a large development of the fault surface. After some preliminary studies, a multicomponent nickel-based alloy with the composition 9Al–14Ti–3.5Cr–73.5Ni (atomic per cent) was found to be appropriate. After a compression test (740 °C; 460 MPa; test duration, 2.5 h), many interacting planar faults could be observed, some of them forming "exotic" geometries such as pyramids (Fig. 7, columns A and B). The pyramidal planes are formed by {111} planes along which SESFs generally lie (*e.g.* R_1, R_2, R_3); R_4 is, however, an FEIS. These faults and the stair-rod dislocations can be identified by the computed image technique, *e.g.* dislocation ab in Fig. 8(b). The derived Burger's vectors are (1/3)⟨013⟩ for ab, (1/3)⟨100⟩ for cd and (1/3)⟨101⟩ for mn. The other SRDL defects have Burger's vectors belonging to one of these three vectors. It should be noted that the Burger's vector (1/3)⟨013⟩ is an exceptionally large vector, larger than the lattice parameter of the cubic cell.

In the deformed precipitates of the alloy CMSX2, intersecting planar defects are also observed, giving rise to SRDL defects, *e.g.* BH in Fig. 1, at the common

edge of the faults F1 and F2. The analysis of the a fringes leads to the determination of the rigid body displacement attached to the planar defects F1 and F2. The contrast of defects F1 and F2 is similar to that of SESFs making an obtuse angle, although the widths of the black fringes in the computed images are always smaller than in the experimental images. Because of the difference in the rigid body displacements on F1 and F2, a stair-rod dislocation was expected along the common edge with Burger's vector $(1/3)\langle 020\rangle$. Six bright field images have been taken (Fig. 7, column a) whose contrasts can be compared with those of computed images, for which SESFs are assumed to be linked to a stair-rod dislocation (Fig. 7, column c). In fact, the result is negative since the theoretical images do not fit correctly the black-and-white contrast of the experimental images near the dislocation core. Nevertheless, an attempt was made to approximate the elastic field around the SRDL defect. Reasonably good agreement was found when using a resultant Burger's vector $(1/3)\langle 010\rangle$ for imaging, as can be seen by comparing columns a and b in Fig. 7. No interpretation of such a result has yet been given, but this observation proves that the structure of the planar defect does not only involve SISFs or SESFs. It probably implies the presence of very thin microtwins as shown by Fig. 6. Their true nature will be studied in the future by high resolution TEM.

Acknowledgment

The authors wish to express their thanks to Dr. A. J. Morton (CSIRO Division of Materials Science, Clayton, Victoria, Australia) for the provision of the programme PCTWO87, modified to treat the superpartial dislocation dipoles of Fig. 3.

References

1 A. J. Huis in't Veld, G. Boom, P. M. Bronsveld and J. T. M. de Hosson, *Scr. Metall.*, *19* (1985) 1123.
2 R. Bonnet and C. Derder, *J. Microsc. Spectrosc. Electron.*, *14* (1989) 415.
3 D. P. Pope and S. S. Ezz, *Int. Metall. Rev.*, *29* (1984) 136.
4 J. P. Hirsch, A. Howie, R. B. Nicholson, D. W. Pashley and M. J. Whelan, *Electron Microscopy of Thin Crystals*, Butterworths, London, 1965.
5 A. J. Head, P. Humble, L. M. Clarebrough, A. J. Morton and C. T. Forwood, *Computed Electron Micrographs and Defect Identification*, North-Holland, Amsterdam, 1973.
6 *METPACK Software* (CERTIB, 4 Allée de l'Atrium, 38640 Claix, France).
7 D. Blavette and A. Bostel, *Acta Metall.*, *32* (1984) 811.
8 M. Condat and B. Décamps, *Scr. Metall.*, *21* (1987) 607.
9 P. Caron, T. Khan and P. Veyssière, *Philos. Mag. A*, *57* (1988) 859.
10 R. Bonnet and A. Ati, *Acta Metall.*, *37* (1989) 2153.
11 Y. Q. Sun, P. M. Hazzledine, M. A. Crimp and A. Couret, *Philos. Mag. A*, *64* (1991) 311.